Rev. Téc. Ing. Univ. Zulia. Vol. 37, Nº 2, 160 - 166, 2014

Influence of gravity on heavy particle statistics in turbulent channel and pipe flow at matched Kàrmàn number

María J. Torres, Javier García

Departamento de Ingeniería Energética y Fluidomecánica,
Escuela Técnica Superior de Ingenieros Industriales, Universidad Politécnica de Madrid.
Calle de José Gutiérrez Abascal, 2, Madrid, España. Phone: +34 (91) 3364156, PC: 28008.
maria.torres@alumnos.upm.es

Abstract

In this work, we use large eddy simulations (LES) and Lagrangian tracking to study the influence of gravity on particle statistics in a fully developed turbulent upward/downward flow in a vertical channel and pipe at matched Kàrmàn number. Only drag and gravity are considered in the equation of motion for solid particles, which are assumed to have no influence on the flow field. Particle interactions with the wall are fully elastic. Our findings obtained from the particle statistics confirm that: (i) the gravity seems to modify both the quantitative and qualitative behavior of the particle distribution and statistics of the particle velocity in wall normal direction; (ii) however, only the quantitative behavior of velocity particle in streamwise direction and the root mean square of velocity components is modified; (iii) the statistics of fluid and particles coincide very well near the wall in channel and pipe flow with equal Kàrmàn number; (iv) pipe curvature seems to have quantitative and qualitative influence on the particle velocity and on the particle concentration in wall normal direction.

Keywords: large eddy simulation, solid particles, turbulent channel and pipe flow.

Influencia de la gravedad sobre las estadísticas de velocidad de partículas sólidas inmersas en un flujo turbulento a través de un canal y una tubería con igual número de Kárman

Resumen

En este trabajo se ha usado el modelo de simulación de grandes escalas y un método de seguimiento Lagrangiano, para estudiar la influencia de la gravedad sobre las estadísticas de velocidad de las partículas en un canal y una tubería, ambos con el mismo número de Kárman. Sobre las partículas actúan solo las fuerzas de arrastre y gravedad y su influencia sobre el flujo no es considerada; el flujo de la fase de transporte es turbulento y completamente desarrollado. Nuestros hallazgos confirman que: (i) la gravedad parece modificar en forma cualitativa y cuantitativa la distribución y velocidad promedio de las partículas en dirección normal a la pared; (ii) solo se modifican cualitativamente las estadísticas velocidad de las partículas en dirección axial; (iii) las estadísticas de velocidad del fluido y las partículas coinciden muy cerca de la pared; (iv) la geometría cilíndrica parece influenciar cualitativa y cuantitativamente la velocidad y distribución de partículas en dirección normal a la pared.

Palabras clave: simulación de grandes escalas, partículas sólidas, flujo turbulento.

Introduction

Transport of solids particles suspended in turbulent gas flow occurs in many industrial devices: filters, pneumatic conveying systems. In all of these applications occur complex mechanisms between turbulence and dispersed phase, therefore is very important to know particle velocity statistics and particle distribution. According to previous experimental and numerical studies, the effect of gravity on the statistics of particle velocity and on the behavior of the particle concentration may become as important as the coupled action of particle inertia and fluid turbulence, since particles under action of potential field (e.g., gravity) are disengaged from fluid turbulence. Our reference work was a numerical experiment developed by [1], where the effects of gravity on the statistics of particle velocity and particle concentration, in a turbulent channel flow, were analysed in a systematic way. From this background, we have developed a LES of a fully-developed turbulent flow laden with solid particles in a vertical channel and additionally, we have extended the study to a vertical pipe with the same Kàrmàn number (or Reynolds number based in friction velocity, Re_τ). Our goals are to quantify and compare the statistics of particle velocity, the evolution of particle concentration in time and particle concentration as a function of wall normal distance, for both configurations.

This paper is organized as follows: first, in the methodology section we summarize the details of the LES of the continuous phase and the Lagrangian tracking of solid particles in channel and pipe at matched Kàrmàn number. Then, the most important results obtained in our simulations are shown, finally in the last section, conclusions will be drawn.

Methodology

Simulation of continuous phase motion

The continuous phase is an incompressible fully developed turbulent flow of air (kinematic viscosity $\nu_g = 1.57 \times 10^{-6}$ m^2.s^{-1}, density $\rho = 1.3$ kg.m^{-3}); it has been modelled by means of space- filtering continuity and time-dependent Navier-Stokes equations:

$$\nabla \cdot \bar{u} = 0 . \quad (1)$$

$$\frac{\partial \bar{u}}{\partial t} + \nabla \cdot \left(\bar{u} \otimes \bar{u}\right) = -\nabla \bar{P} + \nabla \bar{T} . \quad (2)$$

where the over-bar indicates a filtered quantity. $\bar{T}$ is the viscous stress tensor defined as

$$\bar{T} = \left(\nu_t + \nu_g\right)\left[\left(\nabla \bar{u}\right) + \left(\nabla \bar{u}\right)^T\right]. \quad (3)$$

where nt is the sub-grid scale eddy viscosity which is calculated using the dynamic Smagorinky model. Computation of the Eulerian velocity field have been made with Charles Pierce's code [2] and incompressible Navier Stokes equations are solved numerically using an implicit filtering. Time integration is based on the fractional step method and a second-order Adams-Bashforth is used for advancement of the convective terms while implicit Crank-Nicholson method is applied for an update of the viscous term. The Poisson equation for pressure is solved using spectral techniques. The time step in wall units imposed by numerical stability requirements (Courant-Friedrich-Levy number: CFL<1) is Dt+ = 0.10.

For the case of channel, the fully developed turbulent flow bounded by two infinite, vertical, flat and parallel walls is simulated; the origin of the coordinate system is located at the channel wall and the *x*, *y* and *z* axes pointing in the streamwise, wall-normal and spanwise directions, respectively. The Reynolds number of flow is $Re_b = 2100$ based on average velocity ($u_b = 1.65$ m.s^{-1}) and half-width channel ($h = 0.02$ m), the Kàrmàn number of channel flow is equal to 150, where friction velocity is $u_\tau = 0.11775$ m.s^{-1}.

For the pipe flow, the origin of the coordinate system is located at the pipe centerline and the coordinates *x*, *r* and θ correspond to the streamwise, radial and azimuthal directions respectively, however the graphics results are represented with respect to $y = R - r$ (y is positive from the wall pipe to the centerline). For vertical pipe flow simulation, the Kàrmàn number match with the channel; in pipe flow u_b has been estimated by using the Prandtl friction law for smooth pipes [3], resulting a Reynolds number of 2152, which is based on estimated average velocity ($u_b = 1.69$ m.s^{-1}), and radius pipe ($R = 0.02$ m). Calculations have been performed on a computational domain of 3770 ×

300 × 1885 wall units in x, y and z directions for channel flow discretized with 192 × 128 × 96 nodes. For pipe flow, we have used a domain of 1885 × 300 × 942 wall units in x, r, θ directions, discretized with 96 × 96 × 64 nodes. A hexahedral grid is used for both domains; points are equally spaced in streamwise and spanwise/azimuthal directions for both channel and pipe, while a non-uniform discretization was used for the wall normal direction in order to obtain a finer grid next to the wall. The grid spacing in wall units is $\Delta x^+=20$ in the streamwise direction and the minimum grid spacing in wall normal direction are $\Delta y^+ = \Delta r^+ =$ 0.8 Periodic boundary conditions are imposed on the fluid velocity field in the axial and spanwise directions and non-slip boundary conditions are enforced at the walls. Both the channel and pipe flow were initialized with a power law profile at the inlet plane respectively with random fluctuations throughout the entire domain. The flow was enforced by a constant wall shear stress. The pressure drop was equal for channel and pipe streamwise direction; therefore channel length should be adjusted to obtain the same pressure drop pipe.

Simulation of discrete phase motion

For the simulation presented here, we have injected the flow domain with O(10^5) pointwise, rigid and spherical particles, whose effect onto the flow has been neglected (one-way coupling). The non-dimensional particle response time is the ratio between the relaxation particle time (τ_p) and the characteristic flow time (τ_f) and it corresponds to the particle Stokes number (St):

$$St = \frac{\tau_p}{\tau_f} = \frac{\rho_p d_p^2}{18\rho\nu_g}\left(\frac{u_\tau^2}{\upsilon_g}\right). \quad (4)$$

In the present study, particles density (ρ_p) and diameters (d_p) were set to 1000 kg.m^{-3} and 228 μm respectively, corresponding to Stokes number equal to 125. Particle motion is described by a set of ordinary differential equations for velocity and position at each time step. We have considered: the density of particles is much larger than the gas density therefore Basset forces and virtual mass can be neglected; also, the influence of fluid velocity fluctuations are not considered; Brownian diffusion can be neglected too (it becomes important for particles smaller than those considered in this paper), therefore, only the body forces are taken into account and acts along the (positive) streamwise direction corresponding to the vertical channel or pipe. With this simplification the following Lagrangian equations for the particle velocity are obtained:

In Cartesian coordinates (channel flow case):

$$\frac{dx_{pi}}{dt} = v_{pi}. \quad (5)$$

$$\frac{dv_{pi}}{dt} = -\frac{\rho}{\rho_p}\frac{3}{4}\frac{C_D}{d_p}\left|\boldsymbol{v}_p - \overline{u}\right|\left(v_{pi} - \overline{u_i}\right) + g_i = -F_{di} + g_i. \quad (6)$$

where: x_{pi} is the particle position, v_{pi} is the particle velocity, $\overline{u}$ is the filtered gas velocity at the particle position, d_p the particle diameter and F_{di} the drag force. The Stokes drag coefficient C_D valid for particles Reynolds number Re_p to about 40 is computed as:

$$C_D = \frac{24}{Re_p}\left(1 + 0.15Re_p^{0.687}\right). \quad (7)$$

In Cylindrical coordinates (pipe flow case) the LHS of Eq. (6) can be rewritten as:

$$\frac{dv_{pi}}{dt} = \frac{d}{dt}\left(U_p\hat{i} + V_p\hat{e}_r + W_p\hat{e}_\theta\right). \quad (8)$$

In this coordinate system, the axial direction is decoupled from the radial and azimuthal direction, therefore:

$$\frac{v_{pi}}{dt} = \frac{dU_p}{dt}\hat{i} + \frac{dV_p}{dt}\hat{e}_r + V_p\frac{d\hat{e}_r}{dt} + \frac{dW_p}{dt}\hat{e}_\theta + W_p\frac{d\hat{e}_\theta}{dt}. \quad (9)$$

where, $\hat{i}$ $\hat{e}_\theta$ are the unit vectors of the cylindrical coordinate system attached to the particle, which is non-inertial. Then, the time derivative of $\hat{e}_r$ and $\hat{e}_\theta$ is not zero and its rotation velocity with respect to the Cartesian reference system with the same origin is $\omega_p = W_p / r_p$. The complete scalar equations of the particle dynamics in cylindrical coordinates are:

$$\frac{dx_p}{dt} = U_p \;;\; \frac{dr_p}{dt} = V_p \;;\; \frac{d\theta_p}{dt} = \frac{W_p}{r_p}. \quad (10)$$

$$\frac{dU_p}{dt} = -F_{dx} + g_x \;;\; \frac{dV_p}{dt} = -F_{dr} + g_r + \frac{W_p^2}{r_p} \;;$$

$$\frac{dW_p}{dt} = -F_{d\theta} + g_\theta - \frac{W_p V_p}{r_p} \qquad (11)$$

where, $F_{dx}, F_{dr}, F_{d\theta}$ are scalar components of drag force. The solutions of equations in r and θ have a singularity in the center of the reference system where the pipe radius goes to zero. In order to avoid this problem, the calculation in this region is conceptually done out of a circle of small but finite radius around the centerline.

At the beginning of simulation, particles were distributed randomly over the computational domain and their initial velocity was set equal to that of fluid in the particle initial position. Periodic boundary conditions were imposed on particles in both streamwise and spanwise directions. The channel and pipe walls are perfectly smooth and elastic collisions were assumed for particles impacting the wall. To calculate particle trajectories in the flow field, we have coupled a Lagrangian tracking routines with LES flow solver. The routines use a tri-linear interpolation method to determinate the fluid velocity at particle position; with this velocity the equations of particle motion are advanced in time using a fourth order Runge-Kutta scheme. The time step used for particle tracking was chosen to be equal to the time step size used for the fluid, also two orders of magnitude less than relaxation time of particle.

Statistics calculation

For the channel, the initial field flow was then run with an artificially high Reynolds number for a 5 flow through times (1 FTT is defined as the time for fluid particles in the middle channel plane to sweep the domain along the streamwise direction). After turbulent flow was established, the Reynolds number was reset to the actual Re = 2100 and allowed to equilibrate for 9 FTT. For the pipe case, the initial field flow was then run with a Reynolds number of 6000 for 5 FTT before decreasing to the target Reynolds number of 2152. When the statistically stationary conditions were achieved statistics were collected for a total of 100 FTT for both configurations. After release particles into the channel and pipe flow, they require a time (equivalent to Stokes number) to reach a local equilibrium condition with the surrounding fluid, an additional time to forget their initial condition and reach a statistically-steady state. In this work, we have made a simulation using the same time intervals reported in [1], we have gathered statistics during a dimensionless time interval Δt^+ = 450 starting at t^+ = 740. This time is sufficient to compute steady-state values of mean particle streamwise velocity and the particle root mean square (*rms*) velocity components; however, the wall normal particle velocity and concentration profiles presented are in transient state or statistically-developing condition.

Results

Statistics of fluid and particles velocities

Here, we analyse the statistics of particle velocity for each flow configuration. Figure 1 shows the mean particle streamwise velocity, as a function of the wall normal coordinate y^+, for particles

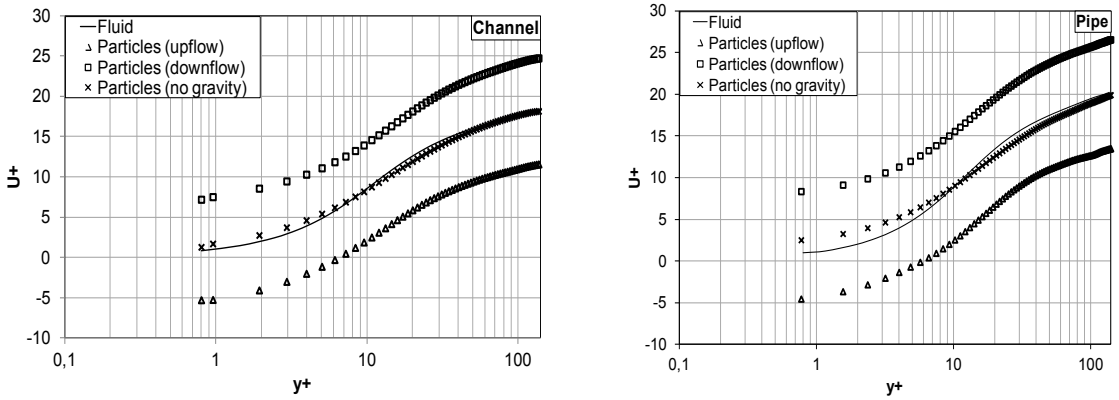

Figure 1. Mean streamwise velocity for fluid and particles.

and each gravity setup. Also, it shows the mean streamwise fluid velocity (solid line) for channel and pipe flow which collapse very well in the region $y^+ < 25$, as expected [4]. In general, if gravity is taken into account, the mean particle streamwise velocity profiles do not overlap with the fluid streamwise velocity profiles; in upflow, particles lag the fluid throughout the semi-width of channel or radius pipe, the opposite occurs in downflow: particles lead the fluid. Particle velocities are very similar up to y^+ 10 for all configurations.

Profiles shown in Figure 2, correspond to the mean wall normal particle velocity and they were computed under statistically-developing condition. Recall that the wall normal velocity is directed toward the wall if negative and away if positive.

For channel and pipe, all particle velocity profiles coincide very well up to ($y^+<5$). The regions of velocity directed to the wall in the pipe flow, are much larger than that in the channel flow for the different gravity configurations; this could occur due to the additional effect of the pipe curvature on the particle motion equation, in which the additional term appears corresponding to the centrifugal force [5]. In upflow, the profiles are wavy and remain negative. In the channel, develops a peak at the upper part of the buffer region ($y^+ \approx 30$, becoming zero from $y^+>90$. In pipe, the profile develops a value peak at the same distance from the channel wall; however this value remains constant up to $y^+ \approx 60$ and then decreases without becoming equal to zero. In channel downward flow, the profile becomes positive outside the buffer region ($y^+>80$) while in pipe downward flow the profile remains negative and its value peak is twice that found in the channel. When gravity is not applied, V^+ remains negative throughout the channel height and pipe radius and their values at the center are roughly equal, however the value peak in the pipe is greater than that in channel.

Figure 3 shows the root mean square of particle velocity along the streamwise direction.

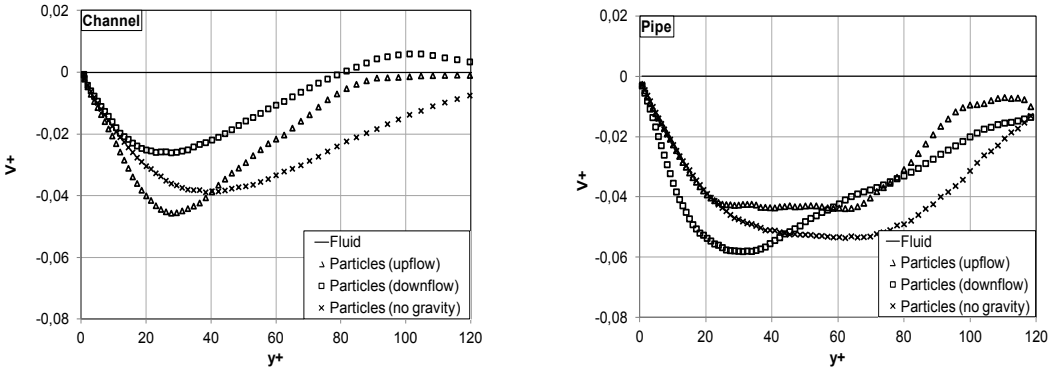

Figure 2. Mean wall normal velocity for fluid and particles.

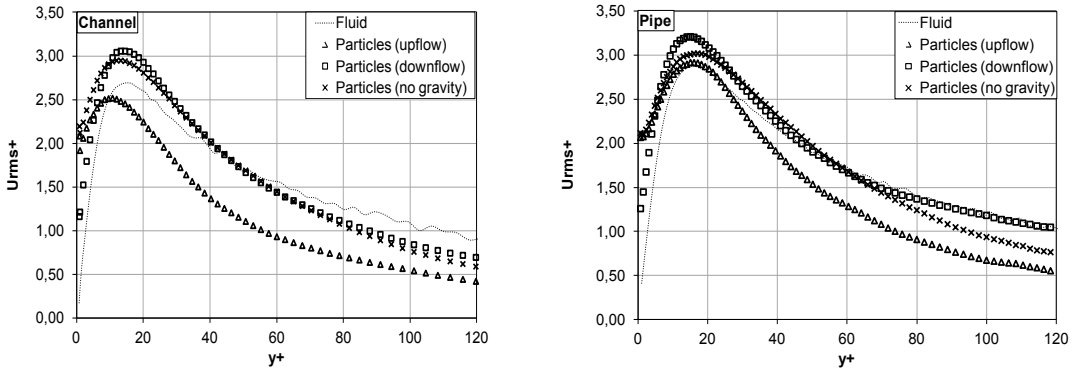

Figure 3. Root mean square of streamwise velocity for fluid and particles.

Comparing both figures, we observe that the peak value of fluid velocity fluctuations is higher in pipe that in channel, though both values occur at the same distance from the wall ($y^+ \approx 16$ roughly). In upward channel flow, the velocity fluctuation is always smaller and reach the peak value closer to the wall than that in no-gravity and downward flow. In the pipe, action of gravity on the fluctuating velocity is more pronounced than in channel, since the corresponding profiles reach higher values throughout pipe radius.

The particle and fluid wall normal velocity fluctuations are depicted in Figure 4. It can be observed that turbulence intensity of the particles is always lower than that corresponding to the fluid for each configuration. The particle velocity profiles coincide very well in the viscous sublayer for channel and pipe. At the center of channel, the effect of gravity direction becomes more pronounced; the same happens at the pipe center.

The behavior of instantaneous and dimensionless particle number distributions (Np/Npo), as a function of the wall-normal coordinate, y^+ at $t+=1190$ are depicted in Figure 5. Starting from the initial uniform distribution of particles, particle concentration has been computed under statistically-developing condition, counting the proportion of particles that fell within each slab in channel and pipe, i.e., by averaging over the streamwise and spanwise directions. For convenience, particle number distribution is normalized by its initial value (Npo).

In the channel, particle concentration profiles set peak at the wall and drop monotonically up to $y^+ \approx 40$ and then rise to their center values; on the other hand, in pipe flow, particle concentration drops monotonically up to $y+ \approx 16$ and then drop abruptly to the centerline.

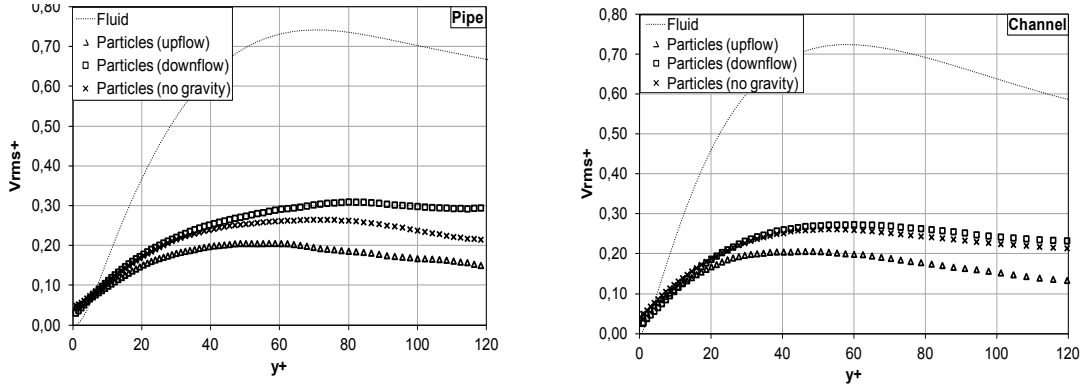

Figure 4. Root mean square of wall normal velocity for fluid and particles.

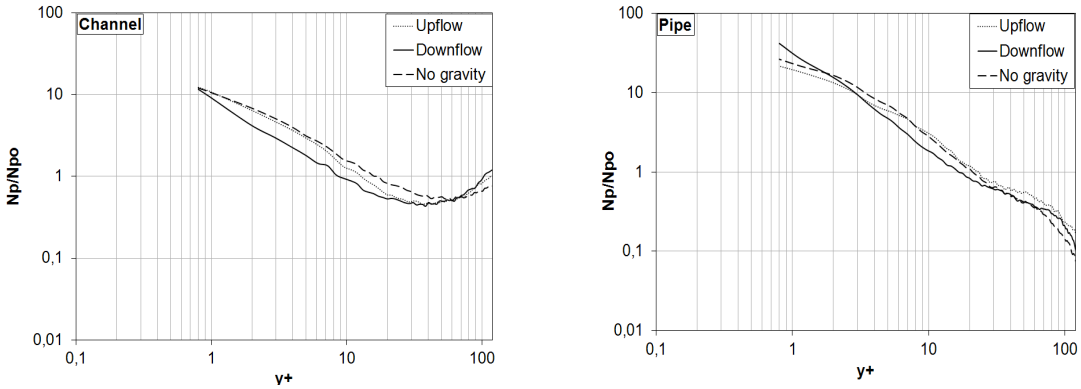

Figure 5. Particle number distribution profiles at $t+ = 1190$.

Conclusions

In this paper, we address the problem of comparing the influence of gravity on particle statistics for turbulent flow in channel and pipe with the same Kàrmàn number. The statistics of particle velocity were compared for both channel and pipe; we observed that they were very similar in channel and pipe flow near the wall so that curvature does not affect the velocity statistics in that region as referred. The behavior quantitative and qualitative of wall-normal velocity was modified, for both geometrical configurations studied. In the straight pipe, that velocity was increased for the action of the centrifugal force owing to pipe curvature. The particle number distribution throughout the pipe radius or half width of the channel does not seem to be strongly affected by gravity. In the pipe and channel, important qualitative differences were observed; the center of the pipe is without particles, so that statistics could not be taken.

References

1. Marchioli, C., Picciotto, M. and Soldati, A.: "Influence of gravity and lift on particle velocity statistics and transfer rates in turbulent vertical channel flow", Int. J. Multiphase Flow Vol. 33, (2007) 227-251.
2. Pierce, C. D. and Moin, P.: "Progress-variable approach for large eddy simulation of turbulent combustion". Report TF-80, Flow Physics and Computation Division, Department of Mechanical Engineering, Stanford University, 2001.
3. Pope, S. B.: "Turbulent Flows", Cambridge University Press, 2000. Engineering, Stanford University, 2001.
4. Monty, J. P., Hutchins, H. C. H. NG., Marusic, I. and Chong, M. S.: "A comparison between pipe, channel and boundary layer flows". J. Fluid Mech., Vol. 632, (2009) 431-442.
5. Marchioli, C., Giusti, A., Salvetti, M. V. and Soldati, A.: "Direct numerical simulation of particle wall transfer and deposition in upward turbulent pipe flow". Int. J. Multiphase Flow, Vol. 29 (6), (2003) 1017-1038.

Recibido el 10 de Febrero de 2013

En forma revisada el 9 de Abril de 2014